Inorg. Chem. **2009**, *48*, 2289−2299

Inorganic Chemistry
Article

Structural Tungsten-Imido Chemistry: The Gas-Phase Structure of $W(NBu^t)_2(NHBu^t)_2$ and the Solid-State Structures of Novel Heterobimetallic W/N/M (M = Rh, Pd, Zn) Species

Hamid Choujaa,[†] Samuel D. Cosham,[†] Andrew L. Johnson,*[,†] Graeme R. Kafka,[‡] Mary F. Mahon,*[,†] Sarah L. Masters,[‡] Kieran C. Molloy,*[,†] David W. H. Rankin,*[,‡] Heather E. Robertson,[‡] and Derek A. Wann[‡]

Department of Chemistry, University of Bath, Claverton Down, Bath BA2 7AY, United Kingdom, and School of Chemistry, University of Edinburgh, West Mains Road, Edinburgh EH9 3JJ, United Kingdom

Received November 4, 2008

The gas-phase (electron diffraction) and solid-state (X-ray) structures of $W(NBu^t)_2(NHBu^t)_2$ (**1**) have been determined. In the gas phase, **1** adopts both C_1 and C_2 conformations in a 69:31 ratio. The solid-state structure is disordered over two equal sites, both showing approximate C_2 conformation as in the gas phase; the imido and amido centers are, however, clearly distinguished. Compound **1** has been used to synthesize novel heterobimetallic derivatives $W(NBu^t)_4[Rh(COD)]_2$ (**3**) and $W(NBu^t)_4[Pd(\eta^3\text{-}C_3H_5)]_2$ (**4**) *via* the dilithiated intermediate $Li_2[W(NBu^t)_4]$ (**2**). In both cases, the $[W(NBu^t)_4]$ moiety bridges the two organometallic fragments. Reaction of **1** with Me_2Zn has produced $[Me(^tBuN)W(\mu\text{-}NBu^t)_2ZnMe(NH_2Bu^t)]$ (**5**). The structures of **3**, **4**, and **5** have been determined. Thermal decomposition of **4** under an autogenerated pressure at 700 °C has formed the hitherto uncharacterized bimetallic alloy WPd_2.

Introduction

Tungsten imido complexes have played an important role in the development of the chemistry of W−N containing compounds[1] and, in more recent years, have been featured in materials chemistry research focused on the formation of tungsten nitride.[2,3] The parent compounds in this class, the mixed imido(amido) species $W(NR)_2(NHR)_2$, were first described by Nugent and Harlow (R = Bu^t),[4,5] although their chemistry owes much to the work of Wilkinson *et al*., who first isolated $Li_2[W(NBu^t)_4]$[6] and utilized this salt to prepare other heterobimetallic imido complexes.[7,8]

The all-nitrogen coordination sphere about tungsten, along with the presence of two strong W═N bonds, has prompted use of $W(NR)_2(NHR)_2$ and its derivatives for the formation of WN in both particulate and thin-film forms.[9−11] Various reports are available dealing with thermal decomposition pathways,[12] thermolysis under different atmospheres,[13] and chemical vapor deposition (CVD) of these compounds.[14−16] Somewhat surprisingly, therefore, the structural chemistry of both $W(NR)_2(NHR)_2$ and the development of bimetallic complexes (which may prove useful precursors to mixed-metal nitrides) have been largely dormant for many years. The solid-state structure of $W(NPr^i)_2(NHPr^i)_2$ has been

* To whom correspondence should be addressed. E-mail: A.L.Johnson@bath.ac.uk (A.L.J.), M.F.Mahon@bath.ac.uk (M.F.M.), chskcm@bath.ac.uk (K.C.M.), dwhr01@holyrood.ed.ac.uk (D.W.H.R.).
† University of Bath.
‡ University of Edinburgh.

(1) Nugent, W. A.; Haymore, B. L. *Coord. Chem. Rev.* **1980**, *31*, 123.
(2) McElwee-White, L. *Dalton Trans.* **2006**, 5327.
(3) Potts, S. E.; Carmalt, C. J.; Blackman, C. S.; Leese, T.; Davies, H. O. *Dalton Trans.* **2008**, 5730.
(4) Nugent, W. A. *Inorg. Chem.* **1983**, *22*, 965.
(5) Nugent, W. A.; Harlow, R. L. *Inorg. Chem.* **1980**, *19*, 777.
(6) Danopoulos, A. A.; Wilkinson, G.; Hussain, B.; Hursthouse, M. B. *J. Chem. Soc., Chem. Commun.* **1989**, 896.
(7) Danopoulos, A. A.; Wilkinson, G.; Hussain-Bates, B.; Hursthouse, M. B. *J. Chem. Soc., Dalton Trans.* **1990**, 2753.
(8) Danopoulos, A. A.; Wilkinson, G.; Sweet, T. K. N.; Hursthouse, M. B. *Polyhedron* **1994**, *13*, 2899.
(9) Becker, J. S.; Gordon, R. G. *Appl. Phys. Lett.* **2003**, *82*, 2239.
(10) Becker, J. S.; Suh, S.; Wang, S.; Gordon, R. G. *Chem. Mater.* **2003**, *15*, 2969.
(11) El-Kadri, O. M.; Heeg, M. J.; Winter, C. H. *Dalton Trans.* **2006**, 1943.
(12) Yang, Y.-W.; Wu, J.-B.; Wang, J.; Lin, Y.-F.; Chiu, H.-T. *Surf. Sci.* **2006**, *600*, 743.
(13) Currie, A. L.; Howard, K. E. *J. Mater. Sci.* **1992**, *27*, 2739.
(14) Crane, E. L.; Chiu, H.-T.; Nuzzo, R. G. *J. Phys. Chem. B* **2001**, *105*, 3549.
(15) Tsai, M. H.; Sun, S. C.; Chiu, H. T.; Chuang, S. H. *Appl. Phys. Lett.* **1996**, *68*, 1412.
(16) Chiu, H.-T.; Chuang, S.-H. *J. Mater. Res.* **1993**, *8*, 1353.

10.1021/ic8021134 CCC: $40.75
Published on Web 01/23/2009

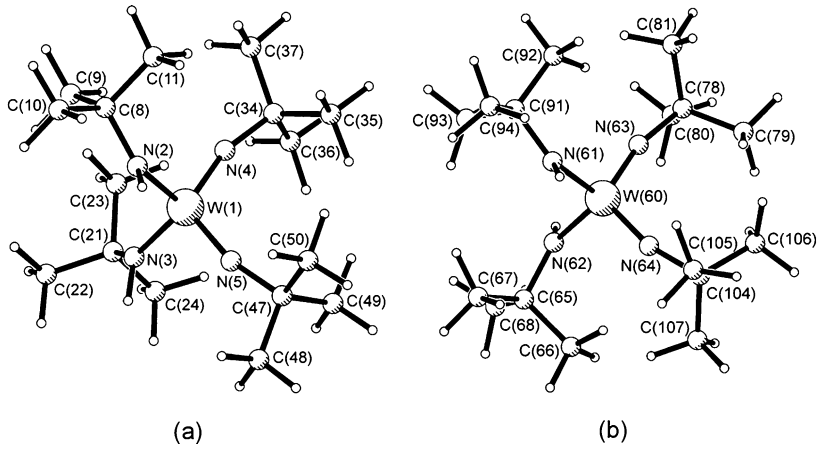

Figure 1. Gas-phase molecular structures of the two conformers of $W(NBu^t)_2(NHBu^t)_2$: (a) conformer 1 with C_1 symmetry and (b) conformer 2 with C_2 symmetry.

reported and is a dimer,[17] while that of the Bu^t analogue has only been the subject of a footnote because of a problem of disorder, though it is believed to be monomeric.[4,18] Furthermore, since the early work of Wilkinson *et al*., which elucidated the structures of $Li_2[W(NBu^t)_4]$[6,7] and $[W_2Cu(NBu^t)_2(\mu\text{-}NBu^t)_6(NHBu^t)_2][BF_4]$,[7] only the structure of $Sn[W(\mu\text{-}NBu^t)_2(NBu^t)_2]$[19] has been added; mixed-metal species, which arise from the replacement of one or more ligands (often the more labile amido groups), do supplement these reports, for example, $W[(\mu\text{-}NBu^t)_2(MX_2)]_2$ (X = Cl, Me; M = Al, Ga)[7] and $W(NBu^t)(NH_2Bu^t)[O(Ph_2SiO)_2]_2$.[20]

In this paper we report on the structure of $W(NBu^t)_2(NHBu^t)_2$ in the gas phase (which is of central importance to CVD studies) and in the solid state, and on the use of this compound to generate the novel heterobimetallic species $W(\mu\text{-}NBu^t)_4[Pd(\eta^3\text{-}C_3H_5)]_2$, $W(\mu\text{-}NBu^t)_4[Rh(\eta^4\text{-}COD)]_2$ and $Me(^tBuN)W(\mu\text{-}NBu^t)_2ZnMe(NH_2Bu^t)$, each of which has been crystallographically characterized. Preliminary exploitation of these species in materials chemistry has shown that $W(\mu\text{-}NBu^t)_4[Pd(\eta^3\text{-}C_3H_5)]_2$ decomposes to the hitherto unknown bimetallic alloy WPd_2 when decomposed at 700 °C under an autogenerated pressure.

Experimental Section

All manipulations were carried out under an atmosphere of dry argon using standard Schlenk and glovebox techniques. Solvents were purified by conventional procedures and distilled prior to use.

Solution ^1H and ^{13}C NMR experiments were performed at ambient temperature using a Brüker Advance-300 MHz FT-NMR spectrometer (University of Bath). ^1H NMR chemical shifts are referenced to Me_4Si. All chemical shifts are in parts per million and coupling constants in hertz. Elemental analyses were performed using an Exeter Analytical CE 440 analyzer. Scanning electron microscopy (SEM) was carried out on a JEOL JSM-6310 microscope equipped with an Oxford Instruments ISIS energy-dispersive X-ray spectrometry (EDXS) attachment, while transmission electron microscopy (TEM) used a JEOL 1200EX machine. The starting materials $W(NBu^t)_2(NHBu^t)_2$ (**1**)[5] and $Li_2[W(NBu^t)_4]$ (**2**)[7] were prepared by literature routes. $[(C_3H_5)PdCl]_2$ and $ZnMe_2$ (2 M in toluene) were purchased from Sigma-Aldrich. $[(COD)RhCl]_2$ was purchased from Alfa.

Syntheses. Synthesis of $[\{W(\mu_2\text{-}NBu^t)_4\}\{Rh(COD)\}_2]$ (3). To an ether solution (15 mL) of $Li_2[W(NBu^t)_4]$ (**2**) (1.0 mmol, 0.47 g) at −78 °C was added dropwise an ether solution (10 mL) of $[(COD)RhCl]_2$ (1.0 mmol, 0.50 g). The reaction mixture was allowed to warm to room temperature, with stirring, during which time the solution changed color to dark brown. The mixture was allowed to stir at room temperature for 2 h, after which removal of solvent under reduced pressure resulted in the precipitation of a yellow/brown residue, which was redissolved in a minimum of fresh hexane (10 mL), with gentle heating. The solution was filtered hot to remove insoluble residues. A brown crystalline solid was obtained on standing overnight at −20 °C. The solid was collected by filtration, washed with cold hexane (−78 °C), and dried in vacuo. Yield: 0.77 g, 86%. ^1H NMR (300 MHz, 23 °C), C_6D_6 (δ ppm): 1.38 (s, 36H, $C(CH_3)_3$), 1.86 (m, 8H, *endo*-C*H*), 2.12 (m, 8H, *exo*-C*H*), 5.08 (s, 8H, =C*H*). $^{13}C\{^1H\}$ NMR (100 MHz, δ): 32.2 (CH_2), 36.3 ($C(CH_3)_3$), 65.7 ($C(CH_3)_3$), 74.3 (d, ^1J(C,Rh) = 11 Hz (=CH)). Anal. Found (calcd for $C_{32}H_{60}N_4WRh_2$): C, 43.1 (43.8); H, 6.8 (6.9); N, 6.3 (6.2)%.

Synthesis of $[\{W(\mu_2\text{-}NBu^t)_4\}\{Pd(C_3H_5)\}_2]$ (4). To an ether solution (20 mL) of $Li_2[W(NBu^t)_4]$ (**2**) (2.0 mmol, 0.94 g) at −78 °C was added a suspension of $[(C_3H_5)PdCl]_2$ (2.0 mmol, 0.72 g) in diethylether (15 mL). The reaction mixture was allowed to warm to room temperature overnight, with stirring, during which time the solution changed color to dark brown/green. Removal of solvent under reduced pressure resulted in the precipitation of a brown residue, which was redissolved in a minimum of fresh hexane (10 mL), with gentle heating. The solution was filtered hot to remove insoluble residues. A dark green crystalline solid was obtained on standing overnight at −20 °C. The solid was collected by filtration, washed with cold hexane (−78 °C), and dried in vacuo. Yield: 1.21 g, 79%. ^1H NMR (300 MHz, 23 °C), C_6D_6 (δ ppm): 1.34 (s, 18H, $C(CH_3)_3$), 1.42 (s, 18H, $C(CH_3)_3$), 2.70 (d, 2H, ^3J = 12.0 Hz, *anti*-CH), 2.73 (d, 2H, ^3J = 12.0 Hz, *anti*-CH), 3.99 (dd, 2H, ^2J = 2.4, ^3J = 6.9, *syn*-CH), 4.02 (dd, 2H, ^2J = 2.4 Hz, ^3J = 6.9 Hz, *syn*-CH), 4.89 (tt, 2H, ^3J = 12.0 Hz, ^3J = 6.9 Hz, middle-CH). $^{13}C\{^1H\}$ NMR (100 MHz, δ): 34.6 ($C(CH_3)_3$), 34.7 ($C(CH_3)_3$), 55.7

(17) Chiu, H.-T.; Chuang, S.-H.; Lee, G.-H.; Peng, S.-M. *Polyhedron* **1994**, *13*, 2443.

(18) There is a discrepancy in ref 4 relating to the cell parameters for $W(NBu^t)_2(NHBu^t)_2$, where they are reported erroneously (monoclinic, C2, a = 21.000, b = 7.602, c = 14.852 Å, β = 106.89°). These data probably refer to the compound $(Me_3SiO)_2Cr(NBu^t)_2$, as the crystallographic data quoted for this compound are essentially identical to what we now report for **1**.

(19) De Lima, G. M.; Duncalf, D. J. *Organometallics* **1999**, *18*, 4884.

(20) Gosink, H.-J.; Roesky, H. W.; Schmidt, H.-G.; Noltemeyer, M.; Irmer, E.; Herbst-Irmer, R. *Organometallics* **1994**, *13*, 3420.

(CH_2), 55.8 (CH_2), 63.0 ($C(CH_3)_3$), 63.1 ($C(CH_3)_3$), 109.1 (CH). Anal. Found (calcd for $C_{22}H_{46}N_4WPd_2$): C, 34.6 (34.9); H, 6.1 (6.1); N, 7.3 (7.3)%.

Synthesis of [Me(^{t}BuN)W(μ_2-NBu^t)$_2$ZnMe(NH$_2$Bu^t)] (5). A solution of $ZnMe_2$ (5.5 mL, 2 M) in toluene was slowly added to a solution of freshly sublimed $W(NBu^t)_2(NHBu^t)_2$ (**1**) (2.00 g, 4.25 mmol) in hexane (75 mL) at −78 °C. After warming to room temperature, the solution was stirred for 24 h. The clear solution was then concentrated until crystallization began. Cooling at −20 °C (12 h) gave colorless needles which were collected by filtration at 0 °C and dried in vacuo. Yield 1.75 g, 73%. Mp 76 °C. ^{1}H NMR (C_6D_6, 300 MHz, 298 K, δ ppm): −0.06 (s, 3 H, ZnCH_3), 0.76 (s, 3 H, WCH_3, $J(^{183}W-^1H) = 9$ Hz), 0.90 (s, 9 H, ZnNC(CH_3)$_3$), 1.48 (s, 18H, μ_2-NC(CH_3)$_3$), 1.51 (s, 9H, NH$_2$C(CH_3)$_3$), 1.83 (br s, 2 H, $(CH_3)_3CNH_2$). ^{13}C NMR (C_6D_6, 300 MHz, 298 K, δ ppm): −12.9 (s, ZnCH_3), 6.8 (s, WCH_3), 31.0 [s, NH$_2$C(CH_3)$_3$], 34.0 [s, μ_2-NC(CH_3)$_3$], 36.0 [s, WNC(CH_3)$_3$], 50.1 [s, NH$_2$$C$($CH_3$)$_3$], 62.7 [s, μ_2-NC(CH_3)$_3$], 66.9 [s, WNC(CH_3)$_3$]. Anal. Found (calcd for $C_{18}H_{44}N_4ZnW$): C, 37.9 (38.2); H, 7.8 (7.9); N, 9.1 (9.9)%.

Computational Methods. All calculations were performed using the facilities provided by the National Service for Computational Chemistry Software (NSCCS)[21] employing the Gaussian 03 suite of programs.[22] Detailed references to computational methods and basis sets can be found therein.

A search of the potential-energy surface using the RHF method and the 3-21G* basis set on all atoms located two conformers of $W(NBu^t)_2(NHBu^t)_2$. As shown in Figure 1, conformer 1 has C_1 symmetry and conformer 2 has C_2 symmetry. The difference in energy between the conformers was calculated to be sufficiently low so that a substantial amount of each conformer could be expected in the experimental gas-phase sample mixture. Geometry optimizations were then carried out for both of these conformers at the MP2 level using the 6-31G* basis set on H, C, and N and for the LanL2DZ pseudopotential on W. A 6-31G* basis set could not be used for tungsten because Pople style basis sets larger than 3-21G* are not available for elements heavier than xenon. All MP2 calculations were frozen core [MP2(fc)]. Calculations were also performed using density functional theory (DFT) at the B3PW91 level using the 6-311+G* basis set on all atoms except W.

For each conformer, a force field was calculated using analytic second derivatives of the energy with respect to the nuclear coordinates obtained at the B3PW91/LanL2DZ/6-31G* level. These were then used by the program SHRINK[23,24] to provide estimates of the amplitudes of vibration (u_{h1}) and curvilinear vibrational correction factors (k_{h1}) to distances required for the gas-phase electron diffraction (GED) refinement. The force fields were also used to calculate vibrational frequencies for the optimized structures. All calculated frequencies were real, indicating that each structure represented a minimum on the potential-energy surface.

Gas-Phase Electron Diffraction. The Edinburgh GED apparatus[25] was used to collect data from a sample of $W(NBu^t)_2(NHBu^t)_2$ synthesized in Bath. An accelerating voltage of 40 keV was used (wavelength ca. 6.0 pm). Scattering intensities were recorded on Kodak Electron Image film at two nozzle-to-film distances, namely, 97.4 and 260.8 mm, to maximize the scattering angle over which data were collected. Four films were recorded at each nozzle-to-film distance. To obtain suitable vapor pressures, the sample was heated to 423 and 443 K, for the long and short nozzle-to-film distances, respectively. The corresponding nozzle temperatures were 429 and 450 K.

The weighting points for the off-diagonal weight matrices, correlation parameters, and scale factors for both distances are given in Supporting Information (Table S1). Also included are the electron wavelengths determined using the scattering patterns for benzene, which were recorded immediately after the sample patterns. The photographic films were scanned using an Epson Expression 1680 Pro flatbed scanner using a routine method described elsewhere.[26] The data reduction and least-squares refinement were carried out using the ed@ed program,[27] using the scattering factors of Ross et al.[28]

Crystallography. Experimental details relating to the single-crystal X-ray crystallographic studies are summarized in Table 1. For all structures, data were collected on a Nonius Kappa CCD diffractometer at 150(2) K using Mo Kα radiation ($\lambda = 0.71073$ Å). Structure solution followed by full-matrix least-squares refinement was performed using the X-seed 2.0 suite of programs throughout.[29] Corrections for extinction were made in the cases of **1**, **4**, and **5**; absorption corrections were made for **1**, **3**, **4**, and **5**.

The determination of the structure of **1** proved the most challenging. Initial attempts at structure solution were hampered at the space group assignment stage. The dominance of the tungsten (located on a crystallographic two-fold axis) almost gave rise to a "special absence" that indicated lattice centering. After this condition was eliminated, there was still some minor ambiguity between *Pncn* and *Pbcn*. A credible solution could be found in the former, which incorporated total ligand disorder, but convergence was poor. The space group as presented provided the optimal convergence and weighting scheme and is in agreement with the proposal in an earlier report[4] that N(1) and N(2) are disordered in a 50:50 ratio with N(1A)/N(2A); this disorder precluded reliable location of the hydrogens attached to N(1A) and N(2A), and consequently, these have been omitted from the refinement. A consequence of the nitrogen disorder became manifest in that C(2)−C(4) and C(6)−C(8) were also modeled at split sites, in a 50:50 ratio.

Crystals of **3** crystallized in the chiral space group of $P2_1$. The structure refined with a Flack parameter of 0.203(5), which, while deviating from zero, is consistent with the assigned absolute configuration. We attribute the deviation from zero to difficulties in the absorption correction as a result of the presence of three heavy atoms.

(21) National Service for Computational Chemistry Software (NSCCS), http://www.nsccs.ac.uk.

(22) Frisch, M. J. ; Trucks, G. W.; Schlegel, H. B.; Scuseria, G. E.; Robb, M. A.; Cheeseman, J. R.; Zakrzewski, V. G.; Montgomery, J. J. A.; Stratmann, R. E.; Burant, J. C.; Dapprich, S.; Millam, J. M.; Daniel, A. D.; Kudin, K. N.; Strain, M. C.; Farkas, O.; Tomasi, J.; Barone, V.; Cossi, M.; Cammi, R.; Mennucci, B.; Pomelli, C.; Adamo, C.; Clifford, S.; Ochterski, J.; Petersson, G. A.; Ayala, P. Y.; Cui, Q.; Morokuma, K.; Rega, N.; Salvador, P.; Dannenberg, J. J.; Malick, D. K.; Rabuck, A. D.; Raghavachari, K.; Foresman, J. B.; Cioslowski, J.; Ortiz, J. V.; Baboul, A. G.; Stefanov, B. B.; Liu, G.; Liashenko, A.; Piskorz, P.; Komaromi, I.; Gomperts, R.; Martin, R. L.; Fox, D. J.; Keith, T.; Al-Laham, M. A.; Peng, C. Y.; Nanayakkara, A.; Challacombe, M.; Gill, P. M. W.; Johnson, B.; Chen, W.; Wong, M. W.; Andres, J. L.; Gonzalez, C.; Head-Gordon, M.; Replogle, E. S.; Pople, J. A. *Gaussian 03*; Gaussian, Inc.: Wallingford, CT, 2004.

(23) Sipachev, V. A. *J. Mol. Struct. (THEOCHEM)* **1985**, *121*, 143.

(24) Sipachev, V. A. *J. Mol. Struct.* **2001**, *567*, 67.

(25) Huntley, C. M.; Laurenson, G. S.; Rankin, D. W. H. *J. Chem. Soc., Dalton Trans.* **1980**, 954.

(26) Fleischer, H.; Wann, D. A.; Hinchley, S. L.; Borisenko, K. B.; Lewis, J. R.; Mawhorter, R. J.; Robertson, H. E.; Rankin, D. W. H. *Dalton Trans.* **2005**, 3221.

(27) Hinchley, S. L.; Robertson, H. E.; Borisenko, K. B.; Turner, A. R.; Johnston, B. F.; Rankin, D. W. H.; Ahmadian, M.; Jones, J. N.; Cowley, A. H. *Dalton Trans.* **2004**, 2469.

(28) Ross, A. W.; Fink, M.; Hilderbrand, R. *International Tables for Crystallography*; Kluwer Academic Publishers: Dordrecht, 1992.

(29) Barbour, L. J. *J. Supramol. Chem.* **2001**, *1*, 189.

Table 1. Crystal Data and Structure Refinement Details for **1**, **3**, **4**, and **5**

	(**1**)	(**3**)	(**4**)	(**5**)
empirical formula	$C_{16}H_{36}N_4W$	$C_{32}H_{60}N_4Rh_2W$	$C_{22}H_{46}N_4Pd_2W$	$C_{18}H_{44}N_4WZn$
formula weight	470.35	890.51	763.28	565.79
crystal system	orthorhombic	monoclinic	monoclinic	monoclinic
space group	*Pbcn*	$P2_1$	$C2/c$	$P2_1/n$
a, Å	12.7590(3)	10.4380(1)	17.9960(2)	13.7450(2)
b, Å	9.3070(2)	11.6450(2)	9.5250(1)	11.8790(1)
c, Å	18.2440(2)	14.8040(2)	7.6150(1)	15.6730(2)
β, deg		108.135(1)	112.497(1)	95.366(1)
V, Å^3	2166.44(7)	1710.05(4)	2789.64(5)	2547.82(5)
Z	4	2	4	4
ρ_{calcd}, Mg m^{-3}	1.442	1.729	1.817	1.475
μ(Mo Kα), mm^{-1}	5.333	4.335	5.403	5.459
F(000)	944	888	1488	1136
crystal size, mm	0.30 × 0.10 × 0.08	0.40 × 0.30 × 0.10	0.20 × 0.17 × 0.10	0.40 × 0.40 × 0.40
theta range, deg	4.38−30.04	3.35−40.22	3.83−34.96	4.01−30.07
reflections collected	43342	62935	45895	54143
independent reflns, R(int)	3155, 0.0780	21125, 0.1133	6111, 0.0785	7456, 0.0792
reflns obs. [$I > 2\sigma(I)$]	1974	12701	5898	6738
max, min transmission	0.70, 0.26	0.6509, 0.2139	0.6141, 0.4113	0.578, 0.112
goodness-of-fit on F^2	1.005	1.031	1.038	1.106
final $R1$, $wR2$ [$I > 2\sigma(I)$]	0.0304, 0.0708	0.0603, 0.1253	0.0319, 0.0830	0.0257, 0.0624
final $R1$, $wR2$ (all data)	0.0551, 0.0820	0.1274, 0.1502	0.0335, 0.0843	0.0304, 0.0669
Flack parameter		0.203(5)		
largest diff. peak, hole, e Å^{-3}	1.825, −1.662	2.934, −3.462	2.949, −2.370	1.489, −1.367

Other than as above, hydrogen atoms were included in calculated positions except for the hydrogens on N(4) in **5** which were located and refined.

Thermal Decomposition of W(NBu^t)$_4$[Pd(η^3-C$_3$H$_5$)]$_2$ (4). The experiment follows the procedure outlined by Gedanken *et al.*[30] A 0.37 g portion of **4** was introduced into the Swagelok cell at room temperature in a nitrogen-filled glovebox. The filled cell was closed tightly with the two plugs and placed inside an iron pipe in the middle of a tube furnace. The temperature was raised at a rate of 10 °C per minute to 700 °C and held at that temperature for 3 h. The Swagelok fitting was gradually cooled (1 °C per minute) to room temperature (25 °C). A 0.25 g sample of a dark black powder was collected.

Results

Gas-Phase Structure of W(NBu^t)$_2$(NHBu^t)$_2$. Ab Initio Calculations. The presence of a heavy transition-metal atom (W) in a molecule normally results in pure ab initio methods performing poorly, and that is observed here. Table 2 illustrates that the geometries show considerable variation between the MP2 and the B3PW91 levels of theory. The geometry of conformer 2 calculated using B3PW91//LanL2DZ/6-31G* has a W−N bond length that is longer by 2.9 pm than that calculated using MP2, with the W−N(H) bond shorter by 1.2 pm. A related effect can also be seen in the calculated geometries of conformer 1, where the W−N distances are also lengthened by 2.7 and 2.5 pm, although this time there is no significant change to the W−N(H) distances. The N−W−N angles are also affected by the method used. For example, ∠N(63)−W(60)−N(64) increases from 113.8° to 115.9° moving from MP2 to B3PW91, and the overall range of N−W(60)−N angles increases by 2.5°. For both conformers, the only parameters significantly affected by alteration of the level of theory were those involving the tungsten atom.

The Gibbs free energies of the conformers were calculated at the B3PW91/LanL2DZ level of theory with two basis sets, 6-31G* and 6-311+G*, on the non-tungsten atoms. At the 6-31G* level, conformer 2 was found to be lower in energy by ∼10 kJ mol^{-1}, while increasing the basis set to 6-311+G* altered this greatly, giving conformer 2 to be lower in energy by ∼5.5 kJ mol^{-1}. Therefore, it was possible that both conformers would be present in the experimental mixture, so both were included in the model written for the least-squares refinement of the GED data. However, the instability of the calculated energy difference with respect to the basis set meant that the absolute value could not be trusted to give an accurate prediction of the conformational makeup.

Table 2. Comparison of Calculated Parameters for W(NBu^t)$_2$(NHBu^t)$_2$ (**1**) Calculated Using the MP2 and B3PW91 Methods[a]

parameter	MP2//LanL2DZ/6-31G*	B3PW91//LanL2DZ/6-31G*
rW(60)−N	176.6	179.5
rW(60)−N(H)	198.6	197.4
rW(1)−N(4)	174.2	176.9
rW(1)−N(5)	173.6	176.1
rW(1)−N(2)	197.6	197.5
rW(1)−N(3)	197.7	197.6
∠N(63)−W(60)−N(64)	113.8	115.9
∠N(63)−W(60)−N(61)	110.3	111.2
∠N(63)−W(60)−N(62)	104.2	103.8
∠N(4)−W(1)−N(5)	115.2	115.9
∠N(4)−W(1)−N(2)	109.9	110.6
∠N(4)−W(1)−N(3)	109.8	109.6
∠N(5)−W(1)−N(2)	103.5	103.3
∠N(5)−W(1)−N(3)	105.9	105.4
∠N(2)−W(1)−N(3)	111.7	112.6

[a] 6-31G* basis sets were used on all atoms except W, for which the LanL2DZ pseudopotential was used. All distances are in picometers and all angles are in degrees.

GED Refinement. To describe the structure of W(NBu^t)$_2$(NHBu^t)$_2$, a two-conformer model was written, using 42 geometric parameters and comprising seven bond lengths, 20 bond angles, and 15 torsions. A nongeometric parameter to control the relative amount of each conformer in the mixture (p_{43}) was also included.

The equivalent bond lengths calculated for the two conformers were almost identical at the B3PW91 level of theory, and it was therefore determined that average bond-length parameters could be used for both conformers with

(30) Pol, S. V.; Pol, V. G.; Gedanken, L. *Chem.−Eur. J.* **2004**, *10*, 4467.

fixed differences between them. This led to the set of seven bond-length parameters. The W−N distances were described by an average and a difference (p_{1-2}), the latter parameter defining the difference between the average W−N and the average W−N(H) distances. In the case of the C_1 conformer, there was also a small difference (less than 1 pm) between the individual W−N distances, and that was included in the model, using a nonrefining parameter fixed at 0.9 pm. An average and two difference parameters were used to describe the C−C and N−C distances (p_{3-5}). These were defined as follows: p_3 = {[C−C] + [N(2)−C] + [N(4)−C]}/3, p_4 = [N(2)−C] − {[N(4)−C] + (C−C)}/2, and p_5 = [N(4)−C] − (C−C). Ab initio calculations showed that while in principle there are three different C−C distances in each *tert*-butyl group, the differences are so small that there would be no benefit in using more than one parameter to describe all 24 of these. Two further distance parameters were used to describe the H-atom positions, *r*C−H mean (p_6) for the methyl hydrogens and *r*N−H for the two imido hydrogens (p_7).

It was necessary to use different angle parameters for the two separate conformers. For the C_2 conformer (conformer 2), these comprised the average of N(4)−W(1)−N(5) and N(3)−W(1)−N(2), the difference between them (p_{8-9}), and the mean values for ∠W−N−C (p_{10}), ∠W−N(H)−C (p_{11}), ∠W−N−H (p_{12}), ∠N−C−C (p_{13}), and finally ∠C−C−H (p_{14}).

For conformer 1, more parameters were required, since the structure exhibits only C_1 symmetry. To describe the N−W−N angles, five parameters were required. The average of the three N(4)−W−N angles ([N(4)−W(1)−N(2) + N(4)−W(1)−N(3) + N(4)−W(1)−N(5)]/3) was used (p_{21}) along with two differences: the difference between N(4)−W−N(5) and the value of [N(4)−W−N(2)+N(4)−W−N(3)]/2 (p_{22}) and the difference between N(4)−W−N(2) and N(4)−W−N(3) (p_{23}). Two further parameters, an average and a difference, were used for the N(5)−W−N angles: the average of N(5)−W−N(2) and N(5)−W−N(3) (p_{24}) and the difference between them (p_{25}). The average of the two W−N(H)−C angles and the difference between them (p_{28} and p_{29}) and also the average and difference of the two W−N−C angles (p_{26} and p_{27}) were used. The remaining angle parameters used for the C_1 conformer were the average and the difference of ∠W−N−H (p_{30} and p_{31}) and the mean values of ∠N−C−C (p_{32}) and C−C−H (p_{33}).

Different torsional parameters were required for the two different conformers. In the case of the C_2 conformer, these were a single methyl-group torsion (p_{18}), parameters to describe the torsions of the butyl groups within the NBu^t ligands (p_{16}) and within the NHBu^t ligands (p_{17}), and a torsion of the overall NHBu^t groups about the N−W bond (ϕH−N−W−N; p_{15}). To model the N atoms about the central tungsten atom, a further parameter was used, defined as a torsion about the *y* axis (p_{20}), using a point X, defined as the point (0.000, 1.000, 0.000), that is, a point exactly 100 pm from the W atom (which sits at the origin) along the *y* axis. A parameter to describe the drop of the *tert*-butyl groups out of the W−N−H plane was also included (p_{19}). All torsion angles were defined to have the same signs for rotations of the respective groups in the same sense.

For the C_1 conformer, again, more parameters were required. The four ligands to tungsten were labeled groups 1−4, with group 1 including N(4), group 2 including N(5), group 3 including N(3), and group 4 including N(2). A single methyl-group torsion was used (p_{40}), and in this case, individual torsions for each of the four butyl groups (p_{36}, p_{37}, p_{38}, and p_{39}) were used. Individual torsions of the two NHBu^t groups (groups 3 and 4) about the N−W bonds were also used (p_{34} and p_{35}) along with parameters to describe the out-of-plane drop of each of these groups (p_{41} and p_{42}).

Using the Boltzmann equation and taking into account that conformer 1 has double multiplicity, it was calculated (from the energy difference calculated at the B3LYP//LanL2DZ/6-311+G* level) that the relative amounts should be 30% of conformer 1 and 70% of conformer 2. The proportionality parameter, p_{43}, controlling the amount of conformer 2, was therefore fixed at 70% for the initial least-squares refinement.

The starting values for the 42 geometric parameters used in the refinement were taken from the highest level DFT calculation carried out (B3PW91//LanL2DZ/6-311+G*). The model was refined as an r_{h1} structure (using curvilinear distance corrections). In total, all 42 geometric parameters and 10 groups of amplitudes of vibration were refined. Where parameters were not sufficiently well defined to refine to sensible values, restraints were applied in accordance with the SARACEN method.[31−33]

After all parameters and amplitude groups were refined, the parameter describing the amount of C_2 conformer was allowed to change to find the value that best fitted the experimental data. As the refinement program is not currently capable of refining this parameter, this was done by incrementally stepping through different conformer amounts to find the minimum R_G value. The final *R* factor for the refinement was R_G = 0.068 (R_D = 0.046), which was obtained for a conformer ratio of 69.5:30.5 (C_1:C_2). Figure 2 shows the *R*-factor ratio, R_G/R_G(min), plotted against the percentage of conformer 2. As can be seen, the *R* factor increases quite sharply on either side of the minimum at 30.5%. The 95% confidence limit[34] (where R_G/R_G(min) = 1.016) represents two estimated standard deviations, and from this, the uncertainty in this value is less than ±1%.

Table 3 lists important bond lengths, angles, and dihedral angles determined by electron diffraction and their calculated equivalents. Table S2 (Supporting Information) contains the full set of independent parameters refined during the least-squares process. The final radial distribution curve for the refinement is shown in Figure 3. The relationship between the vertical lines (representing individual distances) under the radial distribution curve and the curve itself is worthy

(31) Blake, A. J.; Brain, P. T.; McNab, H.; Miller, J.; Morrison, C. A.; Parsons, S.; Rankin, D. W. H.; Robertson, H. E.; Smart, B. A. *J. Chem. Phys.* **1996**, *100*, 12280.
(32) Brain, P. T.; Morrison, C. A.; Parsons, S.; Rankin, D. W. H. *J. Chem. Soc., Dalton Trans.* **1996**, 4589.
(33) Mitzel, N. W.; Rankin, D. W. H. *Dalton Trans.* **2003**, 3650.
(34) Hamilton, W. C. *Acta Crystallogr.* **1965**, *18*, 502.

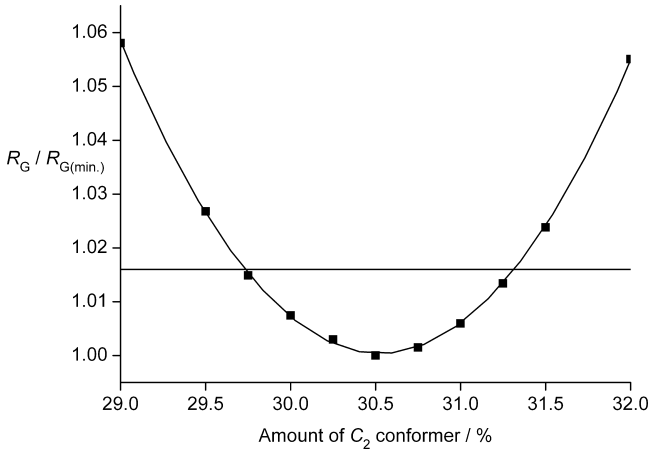

Figure 2. Plot of $R_G/R_G(\text{min})$ against the percentage of conformer 2. The horizontal line shows the 95% confidence limit.

of comment. The two sticks at slightly less than 200 pm do not appear to match the peaks in the radial distribution curve. These sticks represent W−N distances, and because of the very different atomic numbers of these atoms, very different phase shifts occur. The shifts here refer to the local shifts in the phases of the electron waves when they propagate into atomic fields. For distances between atoms with very different atomic numbers, this causes significant splitting of peaks into pairs of peaks. Therefore, the sticks representing the W−N distances lie halfway between the split pairs. This effect was first noticed in a study of UF_6,[35] with the origin of the effect further investigated for ReF_6.[36]

Sets of distances such as N−C and C−C in principle can be different but actually may be identical, so sticks can be superimposed and may appear to be smaller than they really are. Interatomic distances and the corresponding amplitudes of vibration are given in Table S3 (Supporting Information), with the final experimental coordinates for the two-conformer GED analysis given in Table S4 (Supporting Information) and corresponding calculated coordinates and energies in Table S5 (Supporting Information). The least-squares correlation matrix is given in Table S6 (Supporting Information). Figure S1 (Supporting Information) shows the molecular-scattering intensity curve from the refinement.

Comparison of Gas-Phase, Crystal, and Theoretical Structures of $W(NBu^t)_2(NHBu^t)_2$ (1). The solid-state structure of **1** was initially reported as a footnote in a paper by Nugent,[4] citing only cell parameters and commenting that the structure was disordered with the suggestion of the presence of a second phase. We can confirm the original assignment of the space group as *Pbcn* and have now resolved the disorder so that useful geometric data can be reported (Table 4). The structure contains two essentially equivalent tetrahedral molecules in equal amounts because of disorder at each nitrogen position (Figure 4a).

Although disorder precludes the location of the hydrogens of the N−H groups, amido and imido centers are easily distinguished by the W−N lengths and W−N−C angles so that the separate components can be easily disaggregated (Figure 4b,c). As has been established in related W−N(H)R and W═NR systems, the stronger W═N approaches linearity at nitrogen [W(1)−N(1) 1.706(15), W(1)−N(2) 1.708(11) Å, W(1)−N(1)−C(1) 166.4(11), W(1)−N(2)−C(5) 165.6(9)°], while the bond to the amide is weaker [W(1)−N(2A) 1.987(9), W(1)−N(1A) 1.966(11) Å] and more angular [W(1)−N(1A)−C(1) 134.0(7), W(1)−N(2A)−C(5) 130.6(6)°].

Table 3. Selected Refined and Calculated Parameters for the Two-Conformer SARACEN Refinement of $W(NBu^t)_2(NHBu^t)_2$ (**1**)[a]

	parameter	B3PW91[b] (r_e)	SARACEN (r_{h1})	restraint
	Independent			
	both conformers			
p_6	rC−H mean	109.0	110.9(2)	
p_7	rN−H average	101.3	101.3(5)	101.3(5)
	conformer 2			
p_{12}	∠W−N−H conf2	114.7	114.8(10)	114.7(10)
p_{15}	ϕH−N−W−N conf2	114.6	117.0(41)	114.6(50)
p_{16}	Bu^t twist (NBu^t groups) conf2	18.0	61.9(49)	
p_{17}	Bu^t twist ($NHBu^t$ groups) conf2	29.7	61.1(77)	
p_{20}	ϕN−W−X−N[c] conf2	95.1	96.1(18)	
	conformer 1			
p_{32}	∠N−C−C mean conf1	109.2	109.3(4)	109.2(10)
p_{33}	∠C−C−H mean conf1	109.5	112.0(4)	
p_{34}	twist $NHBu^t$ group3 conf1	149.9	151.1(48)	149.9(50)
p_{35}	twist $NHBu^t$ group4 conf1	−135.8	−133.4(36)	−135.8(50)
p_{36}	Bu^t twist group1 conf1	23.0	30.0(29)	23.0(50)
p_{37}	Bu^t twist group2 conf1	18.0	19.3(30)	18.0(30)
p_{38}	But twist group3 conf1	−147.5	−140.8(53)	−147.5(100)
p_{39}	Bu^t twist group4 conf1	32.3	40.9(45)	32.3(100)
p_{42}	Bu^t drop group4 conf1	12.8	12.5(20)	12.8(20)
p_{43}	percentage of conf2[d]	70	31(1)[e]	
	Dependent			
d_1	rN−C	146.8	145.8(5)	
d_2	rN(H)−C	144.0	145.5(8)	
d_3	rC−C average	153.4	153.8(2)	
d_4	rW(1)−N(2)	197.8	199.6(3)	
d_5	rW(1)−N(3)	197.6	199.6(3)	
d_6	rW(1)−N(4)	177.2	176.9(2)	
d_7	rW(1)−N(5)	176.3	175.9(2)	
d_8	rW(60)−N(H)	197.5	199.6(2)	
d_9	rW(60)−N	176.8	176.4(3)	
d_{10}	∠N(2)−W(1)−N(3)	112.6	113.8(22)	
d_{11}	∠N(2)−W(1)−N(4)	110.0	109.0(7)	
d_{12}	∠N(2)−W(1)−N(5)	103.2	103.4(10)	
d_{13}	∠N(3)−W(1)−N(4)	109.6	108.6(7)	
d_{14}	∠N(3)−W(1)−N(5)	105.3	105.6(10)	
d_{15}	∠N(4)−W(1)−N(5)	115.9	116.5(9)	
d_{16}	∠N(61)−W(60)−N(62)	111.2	111.0(11)	
d_{17}	∠N(61)−W(60)−N(63)	111.2	112.0(16)	
d_{18}	∠N(61)−W(60)−N(64)	103.8	103.1(15)	
d_{19}	∠N(62)−W(60)−N(63)	103.8	103.1(15)	
d_{20}	∠N(62)−W(60)−N(64)	111.2	112.0(16)	
d_{21}	∠N(63)−W(60)−N(64)	115.8	115.9(11)	
d_{22}	∠W(1)−N(2)−C(8)	135.1	133.6(10)	
d_{23}	∠W(1)−N(3)−C(21)	138.1	136.5(10)	
d_{24}	∠W(1)−N(4)−C(34)	162.4	162.3(10)	
d_{25}	∠W(1)−N(5)−C(47)	164.9	164.7(10)	
d_{26}	∠W(60)−N−C	163.6	164.0(10)	
d_{27}	∠W(60)−N(H)−C	133.4	133.4(10)	
d_{28}	∠W(1)−N(2)−H(6)	113.5	113.6(10)	
d_{29}	∠W(1)−N(3)−H(7)	111.5	111.6(10)	

[a] All distances are in picometers, angles and torsions are in degrees. Values in parentheses are uncertainties on the last figure. For definitions of parameters, see the text. See Table S2 (Supporting Information) for the full table of parameters. [b] Using the LanL2DZ pseudopotential for W and the 6-31G* basis set for H, C, and N. [c] X is a dummy atom lying in a positive direction on the *y* axis. [d] This parameter was not refined but rather fixed at the value calculated using the Boltzmann equation at the experimental temperature (70%) while the refinement of geometric parameters was in progress. Once this was complete, p_{43} was systematically set to different values, and the resulting *R* factors were plotted to find the optimum conformer mixture. [e] See text for the origin of this uncertainty.

(35) Seip, H. M. *Acta Chem. Scand.* **1965**, *19*, 1955.
(36) Jacob, E. J.; Bartell, L. S. *J. Chem. Phys.* **1970**, *53*, 2231.

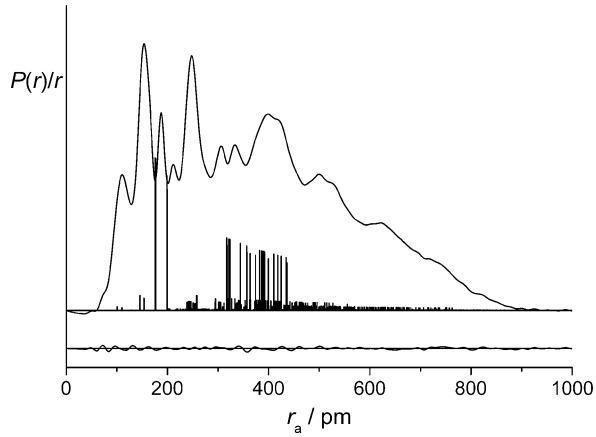

Figure 3. Experimental and difference (experimental minus theoretical) radial distribution curves, $P(r)/r$, for the two-conformer GED refinement of $W(NBu^t)_2(NHBu^t)_2$. Before Fourier inversion, the data were multiplied by $s \times \exp(-0.00002s^2)/(Z_W - f_W)(Z_N - f_N)$.

Table 4. Geometric Data for $W(NBu^t)_2(NHBu^t)_2$ (**1**) in the Solid State[a,b]

molecule 1		molecule 2	
Bond Lengths, Å			
W(1)−N(1)	1.706(15)	W(1)−N(2)	1.708(11)
W(1)−N(2A)	1.987(9)	W(1)−N(1A)	1.966(11)
Bond Angles, deg			
N(1)−W(1)−N(1′)	99.5(10)	N(2)−W(1)−N(2′)	96.6(8)
N(1)−W(1)−N(2A)	110.3(7)	N(2)−W(1)−N(1A)	110.6(6)
N(1)−W(1)−N(2A′)	104.5(5)	N(2)−W(1)−N(1A′)	105.9(5)
N(2A)−W(1)−N(2A′)	124.9(6)	N(1A)−W(1)−N(1A′)	123.9(8)
C(1)−N(1)−W(1)	166.4(11)	C(5)−N(2)−W(1)	165.6(9)
C(1)−N(1A)−W(1)	134.0(7)	C(5)−N(2A)−W(1)	130.6(6)

[a] The structure consists of two molecules in 1:1 disorder. [b] Symmetry operation: $-x$, y, $1/2 - z$.

The conformation adopted by each component resembles the C_2 conformer identified in the gas phase by calculations:

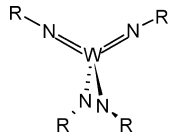

There are minor differences, however, in torsion angles between the calculated C_2 structure and the crystal structure. Specifically, while the W−N(H)−C angles are similar in both (ca. 135°), the Bu^t fragments of the amido groups are rotated more to the left and right [∠C−N(H)−W−N(H), −78.8°] than in the solid [e.g., for the component based on N(1), ∠C−N(H)−W−N(H), 46.3°]. Similarly, the bending of the W═N−C angle away from 180° (to approximately 165°) takes place in the N═W═N plane in the calculated structure [∠C−N═W═N, −2.7°] while in the solid it is in an orthogonal direction [e.g., for the component based on N(1), ∠C−N═W═N, 89.5°].

The molecular structure of $W(NBu^t)_2(NHBu^t)_2$ in the gas phase has also been determined by GED. A two-conformer model gave a much better fit to the electron-diffraction data than either of two single-conformer models, vindicating the computed results that both conformers were present in significant quantities in the experimental sample. The calculated energy difference of approximately 5.5 kJ mol^{-1} (with the C_2 symmetry conformer lower in energy and with half the multiplicity of the less symmetric C_1 conformer) indicated a mixture comprising 30% of conformer 1 and 70% of conformer 2. This is therefore very different from the final conformational composition obtained from the refinement, which suggests a mixture of 69.5% of conformer 1 and 30.5% of conformer 2. There is a sharp increase in R_G on each side of the optimal amount of conformer 2 (Figure 2), indicating that the conformational makeup of the sample mixture is extremely well defined. It can be calculated that the relative amounts of the conformers correspond (at the average experimental temperature of 436.5 K) to a difference in energy of 0.47(7) kJ mol^{-1} (C_1 conformer is lower in energy). The uncertainty in the energy difference between conformers was estimated using the Boltzmann distribution from the energy difference at ±1 standard deviations about the optimum percentage of conformer 2 (see Figure 2). That the two conformers lie so close in energy is not surprising when their relative structures are considered: the only significant difference between the C_1 and the C_2 symmetric forms is in the conformation of a single $NHBu^t$ group, which has only a very small contribution to the overall energy of the molecule. As the two conformers are structurally so similar, very small changes in parameter values were observed while the proportion of each conformer was changed to minimize the R factor. The error in the calculated energy difference between the conformers is not unreasonable for this molecule, for which a very high level of theory and a very large basis set were not feasible. The results demonstrate the importance of doing experiments and not relying solely on theory.

For both conformers, the refined distances and angles are in reasonably good agreement with those calculated using the B3PW91//LanL2DZ/6-311+G* method. The largest discrepancy occurs with the C−C/N−C difference parameter (p_4), which increases from −1.9 to −3.9 pm. This has the effect of bringing the values of the N−C and N(H)−C distances (dependent parameters) much closer together [145.5(8) pm and 145.8(5) pm, compared to 144.0 and 146.8 pm]. The largest difference in angle occurs with the NCC angle in the C_2 symmetry conformer, which refines to 106.7(7)°, compared with the computed value of 109.2°.

Torsional parameters are also generally in good agreement with computed values. However, the torsion angles of the *tert*-butyl groups in the C_2-symmetric conformer differ significantly: 61.9(49)° compared to the calculated 18.0° for the NBu^t groups and 61.1(77)° compared to 29.7° for the $NHBu^t$ groups.

The W−N distances, which make the biggest single contribution to the overall scattering intensity, are in generally good agreement with the values calculated at the B3PW91 level of theory. The most notable difference occurs in the longer W−N(H) distance, which refines to 199.6 pm for both conformer 1 and conformer 2, compared with the calculated values of 197.4 pm for conformer 1 and 197.5 pm for conformer 2. It is comforting to note that the refined value is considerably closer to the sum of the covalent radii

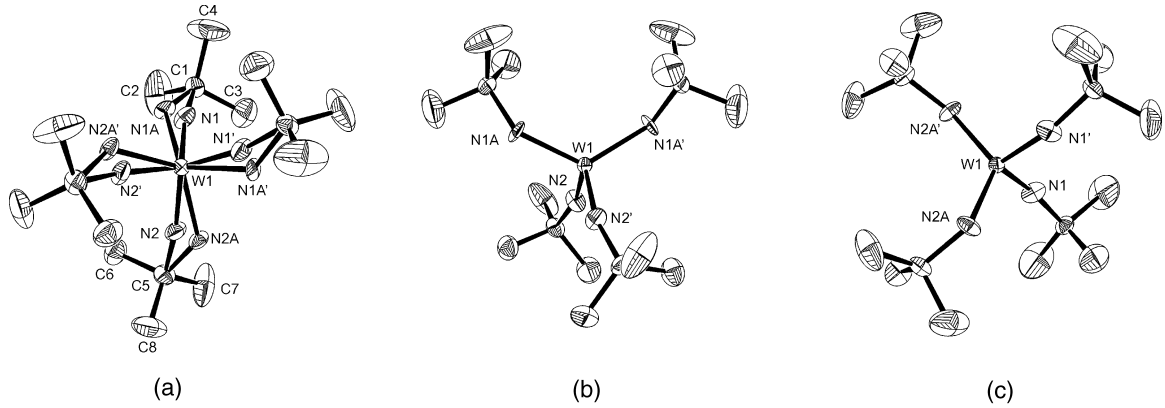

Figure 4. Asymmetric unit of **1** showing the labeling scheme used; thermal ellipsoids are at the 30% probability level. (a) the complete structure showing both components and (b, c) its disaggregated components. In all cases, disorder in the t-Bu groups (split over two sites) has been omitted for clarity. Selected metrical data; symmetry operation: $-x$, y, $1/2 - z$.

of tungsten and nitrogen (200.0 pm).[37] The W−N double-bonded distances refine to within two estimated standard deviations of the calculated values (176.9(2) and 175.9(2) pm for conformer 1, compared with calculated values of 177.2 and 176.3, and 176.4(3) pm for conformer 2, compared with the calculated 176.8 pm).

Synthesis and Structures of Heterobimetallic W/Rh, W/Pd, and W/Zn Compounds. Reaction of the dilithio complex **2** with $[(\eta^4\text{-COD})\text{RhCl}]_2$ in a 1:1 ratio in diethyl ether results in the formation of the trimetal, heterobimetallic complex **3** (eq 1). After stirring for 12 h, the diethyl ether solvent was removed, and extraction into hexane and filtration afforded brown/yellow crystals. ^{1}H NMR spectroscopy of **3** shows the presence of a single resonance at $\delta =$ 1.38 ppm which is attributed to the ^{t}Bu groups, together with the three resonances attributed to the COD ligand, that is, CH_2, *endo*-CH, and *exo*-CH hydrogen atoms, observed in an 8:4:4 ratio, respectively. Evidence points toward the formation of a symmetric system with a high degree of fluxionality.

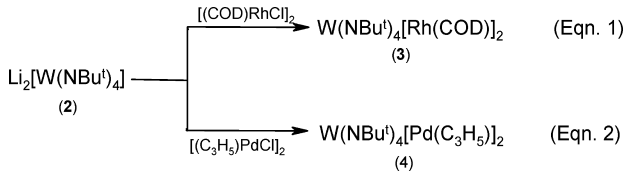

Similar reaction of **2** with $[(\eta^3\text{-}C_3H_5)\text{PdCl}]_2$ (eq 2) afforded green crystals of **4** after extraction and recrystallization from hexanes. As with **3**, ^{1}H NMR spectroscopy of **4** showed the presence of a single resonance attributed to the ^{t}Bu groups ($\delta = 1.34$ ppm), as well as a complex series of multiplets associated with the η^3-coordinated allyl group.[38]

Single-crystal X-ray diffraction studies of both **3** (Figure 5, Table 5) and **4** (Figure 6, Table 6) show that the complexes are built from a central tetrahedral tungsten moiety, formally the $[W(NBu^t)_4]^{2-}$ anion, which coordinates to two organometallic fragments.

The structure of the rhodium complex (**3**) shows the central $[W(NBu^t)_4]$ group coordinating to two $[Rh(\eta^4\text{-COD})]$ units,

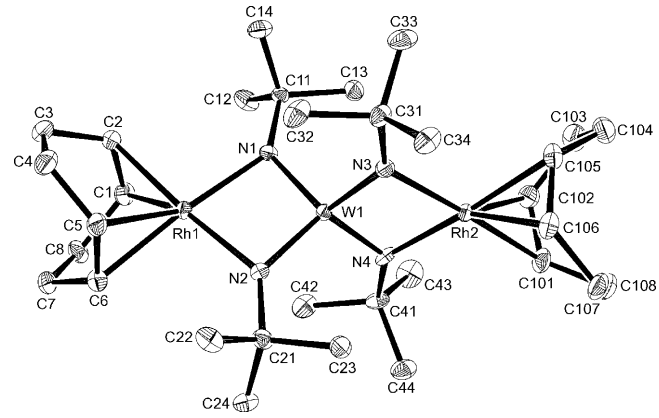

Figure 5. Asymmetric unit of **3** showing the labeling scheme used; thermal ellipsoids are at the 30% probability level.

Table 5. Geometric Data for $W(\mu_2\text{-}NBu^t)_4[Rh(\eta^4\text{-COD})]_2$ (**3**)

Bond Lengths, Å			
W(1)−N(1)	1.865(4)	W(1)−N(3)	1.846(5)
W(1)−N(2)	1.852(4)	W(1)−N(4)	1.881(5)
Rh(1)−N(1)	2.130(4)	Rh(2)−N(3)	2.133(5)
Rh(1)−N(2)	2.133(4)	Rh(2)−N(4)	2.095(5)
Rh(1)−C(1)	2.141(6)	Rh(2)−C(101)	2.183(6)
Rh(1)−C(2)	2.170(6)	Rh(2)−C(102)	2.128(6)
Rh(1)−C(5)	2.117(5)	Rh(2)−C(105)	2.171(6)
Rh(1)−C(6)	2.175(5)	Rh(2)−C(106)	2.121(6)
C(1)−C(2)	1.403(8)	C(101)−C(102)	1.361(9)
C(5)−C(6)	1.409(9)	C(105)−C(106)	1.384(9)
Bond Angles, deg			
N(1)−W(1)−N(2)	102.56(18)	N(2)−W(1)−N(3)	112.3(2)
N(1)−W(1)−N(3)	114.5(2)	N(2)−W(1)−N(4)	114.2(2)
N(4)−W(1)−N(1)	112.1(2)	N(3)−W(1)−N(4)	101.7(2)
N(1)−Rh(1)−N(2)	85.74(16)	N(3)−Rh(2)−N(4)	86.21(15)

which can be considered as possessing square-planar geometry, if the midpoints of each η^2-alkene are taken along with the two μ_2-N. The palladium complex (**4**) is structurally analogous, though of higher symmetry, the two halves of the molecule being related by a two-fold axis bisecting the N(1)−W(1)−N(1′) angle. In **4**, tungsten is again tetrahedral while the palladium is square-planar based on the two μ-N and the terminal carbon atoms of the allyl group [C(1), C(3)]. Both WN_4 tetrahedra are distorted by virtue of the narrow bite angle of each WN_2 unit [**3**: N(1)−W(1)−N(2), 102.56(18) and N(3)−W(1)−N(4), 101.7(2)°], though the planar WN_2M metallacycles are orthogonal to one another.

(37) Emsley, J. *The Elements*; Clarendon Press: Oxford, U.K., 1989.
(38) Mann, B. E.; Pietropaolo, R.; Shaw, B. L. *J. Chem. Soc., Dalton Trans.* **1973**, 2390.

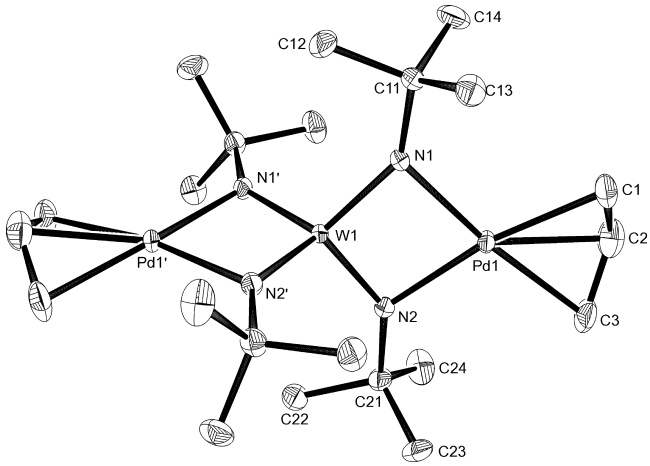

Figure 6. Asymmetric unit of **4** showing the labeling scheme used; thermal ellipsoids are at the 30% probability level. Symmetry operation: $-x$, y, 1/2 $- z$.

Table 6. Geometric Data for $W(\mu_2\text{-}NBu^t)_4[Pd(\eta^3\text{-}C_3H_5)]_2$ (**4**)[a]

Bond Lengths, Å			
W(1)−N(1)	1.8627(19)	Pd(1)−C(1)	2.159(3)
W(1)−N(2)	1.854(2)	Pd(1)−C(2)	2.132(4)
Pd(1)−N(1)	2.113(2)	Pd(1)−C(3)	2.149(3)
Pd(1)−N(2)	2.109(2)	C(1)−C(2)	1.376(6)
		C(2)−C(3)	1.355(6)
Bond Angles, deg			
N(1)−W(1)−N(1′)	115.68(13)	N(1)−Pd(1)−C(2)	136.58(14)
N(1)−W(1)−N(2)	100.63(9)	N(1)−Pd(1)−C(3)	169.40(13)
N(1)−W(1)−N(2′)	114.14(9)	N(2)−Pd(1)−C(1)	170.53(12)
N(2)−W(1)−N(2′)	112.25(13)	N(2)−Pd(1)−C(2)	136.21(15)
N(1)−Pd(1)−N(2)	85.26(8)	N(2)−Pd(1)−C(3)	103.66(12)
N(1)−Pd(1)−C(1)	103.00(12)	C(3)−C(2)−C(1)	122.9(4)
W(1)−N(1)−Pd(1)	86.83(8)	W(1)−N(2)−Pd(1)	87.18(8)
C(11)−N(1)−W(1)	143.29(17)	C(21)−N(2)−W(1)	141.96(17)
C(11)−N(1)−Pd(1)	129.87(16)	C(21)−N(2)−Pd(1)	130.56(16)

[a] Symmetry operation: $-x$, y, 1/2 $- z$.

In both complexes, all four W−N bonds are similar in length [**3**, 1.846(5)−1.881(5) Å; **4**, 1.854(2) and 1.8627(19) Å] and lie midway between W═N distances of terminal imido groups [e.g., 1.751(2) Å in **5**] and W−N single bonds [e.g., 1.931(4) and 1.924(5) Å in (BZP)W(NBu^t)(NHBu^t) (BZP = benzopinnacol)[39] or 1.961(5) and 1.954(4) Å in Cp*W(NO)(NHBu^t)].[40] In both **3** and **4**, the bridging imido nitrogen centers are planar and thus act as π donors to both tungsten and rhodium/palladium.

Me_2Zn was reacted with **1** under similar conditions to those reported earlier by Nugent.[4] In our hands, the reaction was carried out at −78 °C rather than at room temperature, which eliminated the formation of an unidentified by-product which forms as a white precipitate. Our product has essentially the same NMR spectrum as that reported earlier, though our crystallographic study has shown that the original formulation [**5a**: Me(^{t}BuHN)$_2$(^{t}BuN)W(μ-NBu^t)ZnMe] is erroneous and the compound actually generated is Me(^{t}BuN)W(μ-NBu^t)$_2$-ZnMe(NH$_2$Bu^t) (**5**). The product results from methyl group transfer from zinc to tungsten, in a similar manner to the reactions between Me_2Zn and [Cy(H)NAs(μ-NCy)]$_2$;[41] methyl group exchange between Me_2Zn and [W(NPh)(N$_2$NC$_5$-H$_5$)Me]$^+$ has also been reported.[42] The ^{1}H NMR spectra of **5** can be equally well assigned to the correct formulation **5**, with the broad 2H signal being due to the coordinated amine rather than the two amido groups in **5a**. **5** can be thought of as anionic [Me(^{t}BuN)W(NBu^t)$_2$]$^-$ coordinating cationic [MeZn(NH$_2$Bu^t)]$^+$ (**5b**).

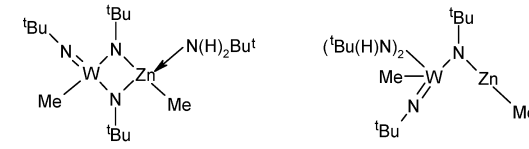

(**5**)

(**5a**)

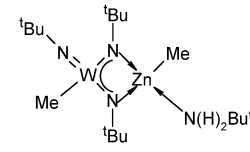

(**5b**)

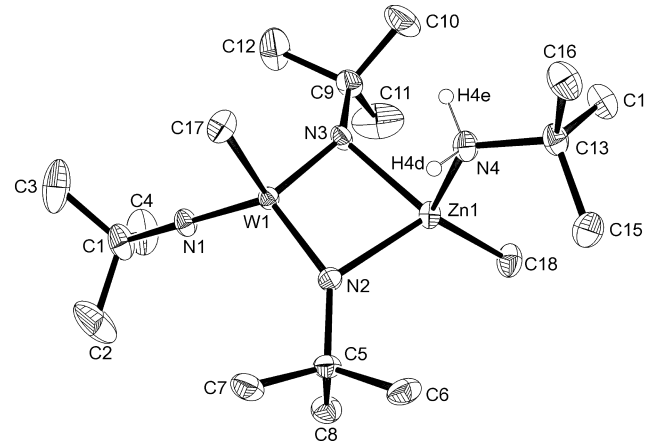

Figure 7. Asymmetric unit of **5** showing the labeling scheme used; thermal ellipsoids are at the 30% probability level.

Table 7. Geometric Data for Me(^{t}BuN)W(μ-NBu^t)$_2$ZnMe(NH$_2$Bu^t) (**5**)

Bond lengths, Å			
W(1)−N(1)	1.751(2)	Zn(1)−N(2)	2.154(2)
W(1)−N(2)	1.838(2)	Zn(1)−N(3)	2.147(2)
W(1)−N(3)	1.841(2)	Zn(1)−N(4)	2.150(3)
W(1)−C(17)	2.149(3)	Zn(1)−C(18)	1.972(3)
Bond Angles, deg			
N(1)−W(1)−N(2)	118.78(11)	N(2)−Zn(1)−N(3)	83.23(8)
N(1)−W(1)−N(3)	119.74(11)	N(2)−Zn(1)−N(4)	97.64(9)
N(1)−W(1)−C(17)	103.07(12)	N(2)−Zn(1)−C(18)	125.25(14)
N(2)−W(1)−N(3)	101.88(10)	N(3)−Zn(1)−N(4)	96.83(10)
N(2)−W(1)−C(17)	106.49(11)	N(3)−Zn(1)−C(18)	126.32(13)
N(3)−W(1)−C(17)	105.65(12)	N(4)−Zn(1)−C(18)	118.85(13)
C(1)−N(1)−W(1)	178.7(2)	C(13)−N(4)−Zn(1)	124.0(2)
W(1)−N(2)−Zn(1)	87.32(8)	W(1)−N(3)−Zn(1)	87.45(9)
C(5)−N(2)−Zn(1)	126.53(18)	C(9)−N(3)−Zn(1)	127.70(19)
C(5)−N(2)−W(1)	141.74(19)	C(9)−N(3)−W(1)	142.5(2)

The structure of **5** is shown in Figure 7 with associated geometric data in Table 7. The location of two hydrogens

(39) Chan, D. M.-T.; Fultz, W. C.; Nugent, W. A.; Roe, D. C.; Tulip, T. H. *J. Am. Chem. Soc.* **1985**, *107*, 251.
(40) Legzdins, P.; Ross, K. J.; Sayers, S. F.; Rettig, S. J. *Organometallics* **1997**, *16*, 190.
(41) Bond, A. D.; Hopkins, A. D.; Rothenberger, A.; Wolf, R.; Woods, A. D.; Wright, D. S. *Organometallics* **2001**, *20*, 4454.
(42) Ward, B. D.; Orde, G.; Clot, E.; Cowley, A. R.; Gade, L. H.; Mountford, P. *Organometallics* **2004**, *23*, 4444.

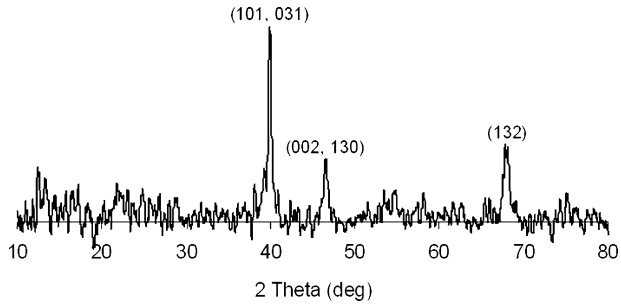

Figure 8. PXRD pattern for the material formed by the RAPET of **4**; lines are indexed by comparison with the data for WPt_2 (PDF 43-1361), details of which are given in Table 8.

on N(4) clearly establishes the presence of a neutral amine coordinated to zinc, whose tetrahedral coordination is completed by a methyl group and nitrogen atoms from two bridging imido moieties. The relative locations of the NH_2 and MeZn moieties are such as to prevent any further intramolecular elimination. The only report of a primary amine adduct of a methylzinc moiety is the unsymmetrical coordinated adamantylaminozinc species [MeZnN(H)R]·THF·H_2NR (R = $C_{10}H_{15}$).[43] Tungsten is similarly tetrahedral in its coordination sphere, the difference being a terminal imido group replaces the coordinated amine in the case of zinc. As expected, the terminal imido group on tungsten is the most tightly bound [W(1)−N(1) 1.751(2) Å] and almost linear [C(1)−N(1)−W(1) 178.7(2)°], similar to that found in Sn[W(μ-NBu^t)$_2$(NBu^t)$_2$].[19] All three Zn−N bonds are longer but are similar to each other in length (*ca.* 2.150 Å) which supports the interpretation of the structure in terms of **5b**, which incorporates three similar N: → Zn interactions. The μ(W−N) bonds [W(1)−N(2) 1.838(2), W(1)−N(3) 1.841(2) Å] follow the same pattern as in **3** and **4** and are also consistent with the presence of partial double-bond character to these bridging W−N bonds. The two methyl groups are disposed trans to each other across the planar WN_2Zn ring.

Materials Chemistry. The thermal decomposition of compounds under an autogenerated pressure (RAPET; reaction under autogenerated pressure at elevated temperatures) has been found to yield core−shell nanoparticles of different types, for example, carbon coated V_2O_3[30,44] or MoO_2,[45] silicon-coated carbon spheres,[30] or carbon sausages with *in situ* WO_3.[46] As an initial exploration of the materials chemistry of heterobimetallic W/M amido complexes, we have studied the RAPET of W(NBu^t)$_4$[Pd(η^3-C_3H_5)]$_2$ (**4**) at 700 °C. EDXS of the decomposition product confirms the presence of both metals, while PXRD (Figure 8; Table 8) shows that the material has limited crystallinity but can be indexed to the pattern for WPt_2 (PDF 43-1361). This implies the formation of WPd_2 in an isomorphous (orthorhombic) form, given the near equivalence of the atomic radii for Pt and Pd (measured as half the M−M distance in the elemental form of the metal: 138.8, 137.6 pm, respectively). While WPt_2 has clearly been characterized previously by PXRD, the only report on WPd_2 relates to the construction of the isothermal cross-sections of the phase diagrams of Pd−Pt−W systems at 1000 °C by physicochemical methods, where orthorhombic phases WM_2 (M = Pt, Pd) were observed in the regions containing >50 atom % of M.[47]

Table 8. PXRD Data for WPt_2[a] and WPd_2[b]

hkl	WPt_2 (*d*, Å)[a]	relative intensity[a]	WPd_2 (*d*, Å)[b]
101	2.2554	100	2.259
031	2.2489	90	
002	1.9533	32	1.953
130	1.9490	58	
132	1.3796	35	1.378

[a] Data taken from PDF 43-1361. [b] See Figure 8; the broad nature of the diffraction lines and the low signal-to-noise ratio does not allow confident resolution of the close (101)/(031) and (002)/(130) pairs.

The mass of product generated (0.25 g) exceeds that expected of pure WPd_2 (theoretical: 0.19 g from 0.3 g **4**), and microanalysis suggests this is predominantly in the form of residual carbon (found: C, 21.4; H, 0.36; N, 0.30%), which is also clearly visible in the EDXS (Supporting Information, Figure S2). The carbon must be in an amorphous form and appears in the SEM in the form of carbon spherules, such as we have observed in similar decompositions, for example, Ti(OEt)$_3$(bdmap) (Hbdmap = bis-(dimethylamino)propanol).[48] However, unlike our previous work, these spherules are generally not of the approximately 1 μm diameter we usually see, and in this case, they are much smaller (*ca.* 100 nm). The morphology of the bulk non-carbonaceous material is unexceptional, with no evidence for the presence of carbon-coated nanomaterials (spheres, wires, etc.; Supporting Information, Figure S3).

Precursor **4**, therefore, appears to act as a single-source precursor for a novel binary alloy, rather than a metal nitride, under RAPET conditions, carrying the stoichiometry of the precursor through to the final material.

Conclusions

The key precursor in tungsten imido chemistry, W(NBu^t)$_2$(NHBu^t)$_2$, adopts two conformations (C_1, C_2 symmetry) in an approximate 70:30 ratio in the gas phase; while in the solid state, a single conformer approximating to the C_2 structure of the gas, though disordered over two sites, has been established. Despite the disorder in the solid state, the W−N imido and amido linkages can be differentiated. W(NBu^t)$_2$(NHBu^t)$_2$ has proved to be a useful starting material in expanding the limited range of known heterobimetallic W/N/M species to include the novel rhodium and palladium species, W(NBu^t)$_4$[Rh(COD)]$_2$ and W(NBu^t)$_4$[Pd(η^3-C_3H_5)]$_2$, respectively. An earlier report on a zinc system has now been reformulated as Me(^{t}BuN)W(μ-NBu^t)$_2$ZnMe(NH$_2$Bu^t) on the basis of X-ray crystallography. These heterobimetallic

(43) Westerhausen, M.; Bollwein, T.; Pfitzner, A.; Nilges, T.; Deiseroth, H.-J. *Inorg. Chim. Acta* **2001**, *312*, 239.
(44) Odani, A.; Pol, V. G.; Pol, S. V.; Koltypin, M.; Gedanken, A.; Aurbach, D. *Adv. Mater.* **2006**, *18*, 1431.
(45) Pol, S. V.; Pol, V. G.; Kessler, V. G.; Seisenbaeva, G. A.; Sung, M.; Asai, S.; Gedanken, A. *J. Phys. Chem. B* **2004**, *108*, 6322.
(46) Pol, S. V.; Pol, V. G.; Kessler, V. G.; Gedanken, A. *New J. Chem.* **2006**, *30*, 370.
(47) Neuimina, S. V.; Zhmurko, G. P.; Kalmykov, K. B.; Sokolovskaya, E. M.; Kuznetsov, V. N. *Vestn. Mosk. Univ., Ser: Khim.* **1992**, *33*, 57.
(48) Hollingsworth, N.; Kanna, M.; Kociok-Köhn, G.; Molloy, K. C.; Wongnawa, S. *Dalton Trans.* **2008**, 631.

compounds have potential application as precursors to ternary metal nitrides, though in an initial experiment carried out in the absence of any additional nitrogen source (e.g., NH_3), the hitherto uncharacterized alloy WPd_2 is formed from decomposition of $W(NBu^t)_4[Pd(\eta^3\text{-}C_3H_5)]_2$ at 700 °C under an autogenerated pressure.

Acknowledgment. We are grateful to the EPSRC for funding the electron-diffraction research (EP/C513649) at Edinburgh and to the National Service for Computational Chemistry Software for the provision of computational resources.

Supporting Information Available: Weighting points for the off-diagonal weight matrices, correlation parameters and scale factors for both nozzle-to-camera distances, interatomic distances and the corresponding amplitudes of vibration, final experimental coordinates for the two-conformer GED analysis, calculated coordinates and corresponding energies, least-squares correlation matrix, the molecular-scattering intensity curve from the refinement, EDXS and SEM images and CIF file. This material is available free of charge via the Internet at http://pubs.acs.org. CCDC 697980−697983 contain the supplementary crystallographic data for compounds **1** and **3**−**5** in this paper. These data can be obtained free of charge from The Cambridge Crystallographic Data Centre via www.ccdc.cam.ac.uk/data_request/cif.

IC8021134